Journal of Sound and Vibration (2001) **241**(4), 541–565
doi:10.1006/jsvi.2000.3315, available online at http://www.idealibrary.com on IDEAL®

HARMONIC BALANCE METHOD USED FOR CALCULATING THE STEADY STATE OSCILLATIONS OF A SIMPLE ONE-CYLINDER COLD ENGINE

F. ALBERTSON

The Marcus Wallenberg Laboratory for Sound and Vibration Research, KTH, Teknikringen 8, 100 44 *Stockholm, Sweden, E-mail: fal@fkt.kth.se*

AND

J. GILBERT

Laboratoire d'Acoustique de l'Université du Maine, UMR CNRS 6613, *IAM, Avenue Olivier Messiaen*, 72085 *Le Mans Cedex* 9, *France, E-mail: joel.gilbert@univ-lemans.fr*

(*Received* 7 *February* 2000, *and in final form* 17 *May* 2000)

A simple piston-constriction-pipe system is analyzed as a first step in the modelling of a "one cylinder cold engine". For the pipe part it is assumed that linear acoustic theory holds, while the source is modelled as non-linear. The interaction between the non-linear source part in the time domain and the linear system part in the frequency domain is examined. To this end, the forced oscillations of the model are calculated by using the harmonic balance method. The assumptions used in the basic model are discussed and an extended model is presented together with simulations showing the practical difference between the two models.

1. INTRODUCTION

In modern society a large number of machines contribute to the total noise pollution. Among them, internal combustion engines are major noise sources due to the increasing density of vehicles on the road. To improve the noise environment, a considerable amount of research is put into areas such as silencers and mufflers for cars, trucks, motorcycles, etc.

For many years the automotive industry has used linear frequency domain method to predict the tailpipe noise. This approach does in some cases give satisfying results, but in general, there are significant discrepancies between the measured final results and the predicted results. In reference [1] Desmons and Kergomard analyzed a simple engine model based on three main assumptions. The source description is linear and time-invariant, the volume velocity is of square signal type and an infinite source impedance is assumed for each cylinder. In the conclusions it is mentioned that the major origin of the discrepancies between theory and experiment lies in these basic assumptions. It does, however, not necessarily has to be the assumption of a linear time-invariant source description alone that is violated.

But the linear frequency domain methods include a lot of knowledge since they have been used for many years. It is therefore interesting to develop methods that take into account the non-linear behaviour of the source but keep the linear description of the rest of the

0022-460X/01/140541 + 25 $35.00/0

system. In this paper, a simple one-cylinder cold engine model is considered. This model is chosen because it shows clear non-linear effects in spite of its simplicity. The aim is to examine if the harmonic balance method, a particular case of Galerkin methods, is an appropriate method for the coupling between a non-linear source description and a linear pipe/muffler system description, to extract solutions for different unknowns and to do parametric studies. Even if this application is a simple cold engine model, the methodology presented is general and can be applied to any acoustic system.

In acoustic applications for engine intake and exhaust systems, three main approaches exist: the linear frequency domain approach, time-variant or time-invariant, the non-linear time-domain approach and the hybrid method approach (see, for example, reference [2] for a review of methods). For very complex systems, it is difficult to find a valid theoretical model. In these cases, two possibilities exist, the use of complex computational programs or measurements of source data. For the computational codes a coupling method has to be applied to perform the interaction between the source and the rest of the system. In measurement cases a source model that allows interaction has to be applied.

The non-linear time-domain methods are in general founded on various numerical simulations of the unsteady flow. The results agree fairly well with experimental results but the methods are very time consuming. These methods also require a good knowledge of engine modelling, such as the combustion process, mechanics of the valve openings, exact knowledge of the complicated geometry, temperature gradients in the system and so on.

In the literature, many different methods have been proposed. Since there is no known analytic solution of the full Navier–Stokes equations, all methods rely on different numerical techniques. For example the non-mesh method (method of characteristics) of Jones and Brown [3], the mesh method proposed by Ferrari and Castelli [4], a finite-volume method from Sapsford *et al.* [5] and a MacCormack scheme method derived by Payri *et al.* [6, 7]. Note that all methods mentioned above are one-dimensional.

On the other hand, the frequency domain, where harmonic solutions to linear systems in the permanent regime are studied, features simple models with short calculation times. The linear frequency domain model is thus interesting and widely used in the development processes of for example exhaust and intake mufflers [8, 9]. However, these methods are based on pure acoustic theory: that is, the source is described as linear and time invariant. The interaction between the engine manifold, the acoustic source, and the exhaust or intake system is therefore poor. In the conclusions of Munjal [8] it is stated that one of the areas where considerable research input is needed is the frequency domain characterization of the engine exhaust source. Davies *et al.* [10] state that the frequency domain approach is a good tool in the development and design processes, as long as a source/pipe-muffler interaction is appropriately included.

Many processes in the engine manifold are clearly non-linear, for example, combustion, supersonic flow in valve openings and large temperature gradients. Since the non-linearities produce different wave shapes for different loads, different exhaust and intake systems will experience different acoustic sources. In order to have a good accuracy in the linear approximation, one therefore needs to determine the source data for each operation point of the engine and for each exhaust and intake system used. Historically, this is done experimentally [11] and it is of course time consuming. One of the advantages with the linear approximation thus disappears. It is, though, very important to mention that even for a simple approximation like this, one finds interesting results [1]. Cases where the prediction of sound in exhaust pipes is good [12–14] are also found.

Suppose that a measurement section is placed sufficiently away from the outlet of the turbo. Then recent studies on the wave propagation in exhaust systems of turbo-charged

diesel engines show that linear wave propagation is a good approximation, see for example references [12–14]. For a cross-section closer to the turbo outlet linear propagation does not hold. This does in general not imply and difficulties in truck applications since the mufflers in the exhaust systems are in general sufficiently away from the turbo outlet. To get a complete description of the system one of course has to include non-linear propagation as well. This has been done in references [10, 16, 17].

A hybrid method, taking the non-linearities of the source into account but keeping the linear description of the exhaust and intake system, is therefore very attractive. This approach increases the accuracy compared to that of the linear model by permitting the source to react differently to different exhaust and intake systems. Such hybrid models have most of the advantages of the linear frequency domain models. The authors think that the results are in general not as accurate as the results from non-linear computational fluid dynamics methods, but substantially shorter calculation times are possible. Several different hybrid methods for predicting the exhaust and intake noise from internal combustion engines have been proposed. Gupta *et al.* [15] have proposed a method for performing the time–frequency domain coupling. Desantes *et al.* [16] as well as Davies *et al.* [10, 17] have proposed hybrid methods for the wave propagation in the exhaust/intake pipes. Here, we focus our attention on the source, i.e., the time–frequency coupling. The main reason for this is that it is possible to use all research experience of linear systems if the pipe/silencer system is considered linear.

Furthermore, recently developed linearity tests can be applied to the experimental source data with only an output signal to determine the degree of non-linearity [18, 19]. These tests can be used to check if a hybrid, or in worst cases, a non-linear method has to be used. In some applications, it is surely found that a linear approximation is sufficient. In reference [19] the proposed linearity tests are applied to loudspeakers, axial flow fans, internal combustion engines both for cars and trucks as well as intake and exhaust systems, and compressors. The results show that the standard loudspeaker and the axial flow fan behave linearly, i.e., a linear source model gives good prediction in a large frequency range. In the case of internal combustion engines, the results show a clear non-linearity in all types of systems. But the prediction of sound is good for the dominating harmonics. According to these results, a hybrid method would probably increase the accuracy. The compressor is according to the linearity tests a non-linear source as well. A hybrid or fully non-linear method should be applied.

One method that is particularly well suited for the time–frequency domain coupling is the harmonic balance technique, a particular case of the Galerkin method. It has been developed to determine the periodic response of non-linear systems in microwave circuits in forced oscillations; see for example references [20, 21]. The method features a short calculation time and it is easy to perform parametric studies.

More recently, the method has been successfully used on self-sustained oscillations in single-reed woodwind instruments [22]. In reference [23] the method has been analyzed to include the stability analysis of the periodic regimes obtained for free and forced oscillations in microwave circuits. Here, the method is herein adopted to forced oscillations in engine-like applications.

In this paper, a simple piston-restriction system, that is a first model of a simple cold engine model, is analyzed with forced oscillations. The system is divided into two parts. One part, regarded as the source part, consists of the piston and the constriction. For this part a non-linear time-domain description is used. The rest of the system is considered as linear acoustics in the frequency domain. The two domains are coupled by the harmonic balance method, which is a specialized method to study time–frequency couplings of periodic systems.

The basic idea of the harmonic balance method is to select an appropriate unknown for a convergence test. The next step is to rearrange the equations, linear or non-linear in the time domain as well as in the frequency domain, in a so-called convergence loop. A new value of the chosen convergence unknown is now calculated and compared to the original value. If the convergence condition is satisfied, one says that a solution has been found. Otherwise, an increment of the convergence unknown is calculated and a new result is calculated by using the defined convergence loop.

The harmonic balance method is found to be a very useful tool for time–frequency domain couplings. It is easy to extend the equations to examine the effects of the assumptions. Furthermore, a parametric study is easily performed and in this paper a lot of results are presented, such as internal pressures, volume flows, densities and so on. As expected, the results show clear non-linear effects. Finally, the result from the simulations are in some sense qualitatively compared to some other published results.

The assumptions used in the model are discussed and an extended model is presented. Furthermore, the parametric study of the basic model indicates more possible extensions.

The outline of this paper is as follows. After a general introduction, the piston–compressor model is described together with other existing models of cold and hot engines given in the literature. Some possible extensions of the model are also given. The next section is devoted to the harmonic balance method applied to the piston-constriction model and the results from numerical simulations. Finally, a discussion and conclusions are given in the last section. In the appendices, the time-domain solution method used to check the results from the harmonic balance method, the different convergence loops used in the harmonic balance and a list of symbols are presented.

2. THE PISTON-CONSTRICTION AND COLD ENGINE MODEL

2.1. MODELS IN THE LITERATURE

A comprehensive review has been given in reference [2]. Non-linear engine models have been used by Payri *et al.* [7] together with non-linear wave propagation in exhaust pipes [6, 24]. In reference [7] a fundamental non-linear model has been used with a thermodynamical description including mass exchanges and heat losses for each cylinder [25]. Combustion has been simulated by use of a simple Watson law [26] which has been fitted to experimental data. The calculation of flow in ducts has been performed fully non-linearly by a MacCormack finite-difference scheme [6]; note though that only the pulsating flows was calculated, i.e., no mean flow was considered. But for all so-called singularities, viz., duct junctions, area changes, mufflers and so on, a quasi-steady model was used. The quasi-steady approach was also used for heat transmission and friction losses in the pipes. In reference [7] a quasi-steady turbine model was also included.

A similar approach has been used by Davies *et al.* [10, 17], where the engine is modelled in the time domain with thermodynamics and non-linear gas dynamics. For the intake/exhaust systems, quasi-linear acoustics was used. In reference [17] it was stated that the analysis of the thermodynamic and non-linear gas components is best performed in the time domain, with appropriate boundary conditions from the passive systems.

In most applications to silencer systems, however, a linear description of the source has been used [1, 8, 11–15]. In all these papers, the standard Thevenin or Norton circuits were used. As an extension to the linear time-invariant source model a shape, somewhat close to a

square for the volume velocity of the different cylinder signals, was used in reference [1]. The noise was analyzed as a first order expansion of the deviation of the signal from a square signal, the time overlap ratio of the cylinder signals and the length ratios of the manifold pipe system.

In recent publications by Boonen *et al.* [27, 28] an extended linear source model is used for a four-cylinder cold engine. They combined the linear source elements with four switch-resistor combinations. This allows the source to be time-variant since the same type of control sequence as the actual valves manages the switches.

The piston-restriction model is based on papers about piston compressors [29–32]. These papers include modelling of the valves as well, but here a simpler model is to be studied.

2.2. THE BASIC MODEL

In this paper, a basic model of a piston-restriction system is used. The system is considered as one-dimensional. It was developed by Bodén [33, 34] to investigate measurement techniques of time-variant sources. Approximately, similar models have been developed in references [35, 36]. In both theses [35, 36], a model of a simple hot engine has been presented. The basic equations used in these models are conservation of mass, conservation of momentum and conservation of energy. Since a cold engine model is to be studied here, the model is based on conservation of mass, conservation of momentum and continuity in volume flow. The actual system, used in the experiments [33], is depicted in Figure 1. This is a piston compressor, where the valve has been removed.

As the valve of the compressor is removed, the piston generates a pulsating flow through the constriction. Note that there is no mean flow, so the sign of the flow alternates. This, however, does not imply that the HBM cannot be used in situations with mean flow. But here, only the system without mean flow is considered. The pipe is considered as linear, i.e., it can be described by an impedance or admittance in the frequency domain. The equations of the rest of the system are written in the time domain and are not linearized. A principal

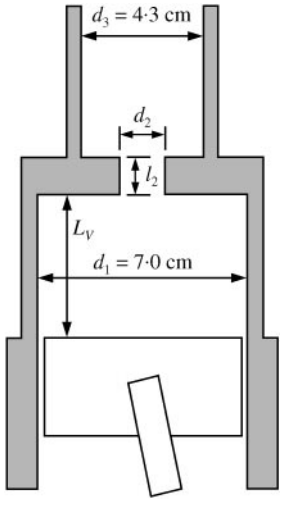

Figure 1. The compressor used in the model. A one-dimensional approximation is used. The source volume is labelled volume 1, the constriction, volume 2 and the pipe, volume 3.

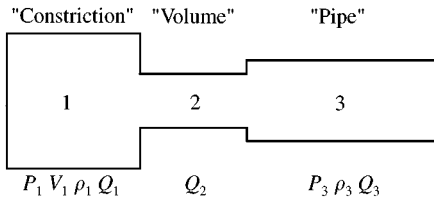

Figure 2. A principal sketch of the system given in Figure 1. The physical unknowns are written below each corresponding section. Regions 1 and 2 are considered as compact, but region 3 can be long. The variables P_3, ρ_3 and Q_3 are thus input variables of the "pipe" (region 3).

sketch of the system is shown in Figure 2 together with the unknowns in each part. We divide the system as shown in Figure 2 into three parts. In each part, the unknowns and constants are indexed with the corresponding number.

The objectives are to calculate the pressure P_3 and volume flow Q_3 at the entrance of pipe 3, where the pipe, which can be a very complicated one, is described by an admittance Y_3 in the frequency domain. To this end, it is assumed that the constriction behaves like a stiff mass plug, that is the density ρ_2 is constant (time independent), while the volume flow $Q_2(t)$ is only time varying. For the junctions, mass conservation and volume flow are supposed to be continuous. The densities $\rho_1(t)$ and $\rho_3(t)$ are assumed to be equal, uniform and have their mean density equal to $\overline{\rho_1} = \overline{\rho_3} = \rho_2 = 1{\cdot}23\ \mathrm{kg/m^3}$. The conditions are supposed to be adiabatic, the flow is assumed to form a jet at the outflow and finally the velocities are assumed to be constant in propagation planes over the duct cross-section. The problem is treated as one-dimensional.

In the rest of the paper, the time dependence is consistently omitted, but the frequency dependence is explicitly included, i.e., $P_3(t) = P_3$ but $P_3\ (\omega) = P_3(\omega)$. (A list of symbols is given in Appendix C.) Now, let V_1 be the volume of volume 1 in Figure 2, and B_1 the boundary of V_1. Note that the size of the volume changes in time according to the piston movement. In each time step one thus integrates over different volumes. Then conservation of mass gives

$$\frac{\mathrm{d}}{\mathrm{d}t}\int \rho_1\,\mathrm{d}V_1 = -\int \rho_1 \mathbf{u}_1 \cdot \mathbf{n}\,\mathrm{d}B_1, \tag{1}$$

at every instant. Here $\mathbf{n}$ is the outward normal, $\mathbf{u}_1$ is the velocity and ρ_1 the density. As uniform density is assumed in volume 1 the integral on the left-hand side becomes $\int \rho_1\,\mathrm{d}V_1 = m_1$. The only outflow is $\rho_2 Q_2$ and equation (1) becomes

$$\mathrm{d}m_1/\mathrm{d}t = -\rho_2 Q_2. \tag{2}$$

One-dimensional unknowns imply that the equation of conservation of momentum is

$$\rho\ \mathrm{D}u_x/\mathrm{D}t = -\partial P/\partial x.$$

Here u_x is the velocity is the x direction and P is the total pressure. The derivative $\mathrm{D}/\mathrm{D}t$ is called the material derivative, which is the rate of change "following the fluid". Integration between planes 1 and 21 defined in Figure 3 leads to

$$\rho_1 \int \frac{\mathrm{D}u_x}{\mathrm{D}t}\mathrm{d}x = -\int \frac{\partial P}{\partial x}\,\mathrm{d}x. \tag{3}$$

In evaluating these integrals it is assumed that $u_x = u_{21}(t)h(x)$, which is a common assumption for deriving acoustic end corrections. Note that the function $h(x)$ is without

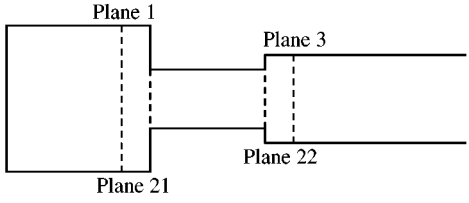

Figure 3. Definition of calculation planes used in the derivation. Note that planes 1 and 21 are as close as possible. The same holds for planes 22 and 3.

dimension. Since one-dimensional unknowns are assumed, u_{21} denotes the mean value of the velocity in propagation plane 21, orthogonal to the x-axis. After integration, the equation becomes

$$\rho_2 \frac{\mathrm{d}u_{21}}{\mathrm{d}t}\,\delta_1 + \frac{\rho_1}{2}(u_{21}^2 - u_1^2) = P_1 - P_{21}, \tag{4}$$

where δ_1 is the acoustic end correction with a typical value of $0{\cdot}82d_2$ for baffled pipes. The velocities u_1 and u_{21} are the mean fluid velocities at planes 1 and 21 and P_1 and P_{21} are the corresponding pressures. The densities ρ_1 and ρ_3 are defined in Figure 2.

Since the flow alternates, the problem is divided into two subproblems. Upon assuming that the fluid in the constriction is incompressible and equivalent to that caused by a piston, (see Figure 4) the sound transmission through the constriction for $u_{21} > 0$ is given by

$$P_{21} - P_{22} = \frac{\mathrm{d}}{\mathrm{d}t}(\rho_2 l_2 u_2) = \rho_2 l_2 \frac{\mathrm{d}u_2}{\mathrm{d}t}, \tag{5}$$

where the calculation planes are given in Figure 3. The length l_2 is the length of the constriction; see Figure 2. The flow is assumed to separate from the wall at the end of the constriction forming a free jet. Then the very unstable free jet tends to break down into vortex rings that are dissipated in the "turbulent mixing zone". After this zone, even if the section area is much greater than the area of the constriction, no recovery of the pressure is assumed to occur. Continuity in pressure thus gives $P_{22} = P_3$. The volume flow Q_2 is assumed to have only time dependence and consequently $u_{21} = u_{22} = u_2$. This gives, together with equation (5),

$$P_1 - P_3 = \frac{\rho_1}{2}(u_2^2 - u_1^2) + \rho_2 (l_2 + \delta_1)\frac{\mathrm{d}u_2}{\mathrm{d}t}. \tag{6}$$

For the case of $u_2 < 0$ a similar procedure yields

$$P_1 - P_3 = -\frac{\rho_3}{2}(u_2^2 - u_3^2) + \rho_2 (l_2 + \delta_3)\frac{\mathrm{d}u_2}{\mathrm{d}t}, \tag{7}$$

where subscript 3 denotes quantities in volume 3.

To relate the density ρ_1 and the pressure P_1 a polytropic process is used, i.e.,

$$P_1 = P_0 (\rho_1/\rho_0)^n. \tag{8}$$

The constant $n = 1{\cdot}4$ is the polytropic index.

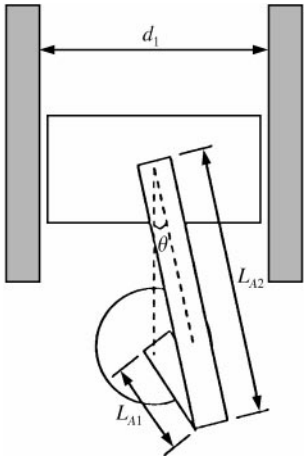

Figure 4. Detailed picture of the piston movement.

Finally, acoustic equations are assumed to hold in the input of pipe 3. It is then convenient to describe them by an impedance/admittance relation in the frequency domain. This means of course that very complicated "pipes" such as complete exhaust systems can easily be applied. Here,

$$Q_3(\omega) = Y_3(\omega)P_3(\omega) \tag{9}$$

Continuity in volume flow in the junctions, equations (2, 6–9), gives the basic model used in this paper. In summary, the equations giving the basic model of the piston-restriction system are

$$P_1 - P_3 = \begin{cases} \dfrac{\rho_2}{2} Q_3^2 \left(\dfrac{1}{S_2^2} - \dfrac{1}{S_1^2}\right) + \dfrac{\partial Q_3}{\partial t} \dfrac{\rho_2}{S_2} (\delta_1 + l_2), & Q_3 > 0 \\ -\dfrac{\rho_2}{2} Q_3^2 \left(\dfrac{1}{S_2^2} - \dfrac{1}{S_3^2}\right) + \dfrac{\partial Q_3}{\partial t} \dfrac{\rho_2}{S_2} (\delta_3 + l_2), & Q_3 < 0 \end{cases} \tag{10}$$

$$\frac{\mathrm{d}}{\mathrm{d}t}(V_1 \rho_1) = -\rho_3 Q_3, \qquad P_1 = P_0(\rho_1/\rho_0)^n, \tag{11, 12}$$

$$Q_3(\omega) = Y_3(\omega)P_3(\omega). \tag{13}$$

The oscillating volume $V_1(t)$ provides the driving force and is closely linked to the movement of the piston. From the specification of the piston movement the oscillating volume is found to be

$$V_1 = S_1 L_v + S_1 L_{A1} \left(1 + \cos(\omega t) + \frac{L_{A2}}{L_{A1}} \left[1 - \sqrt{1 - \left(\frac{L_{A1}}{L_{A2}}\right)^2 \sin^2(\omega t)}\right]\right), \tag{14}$$

where L_{A1} and L_{A2} are the lengths of the axis specified in Figure 2, ω is the angular frequency, S_1 is the area of the pipe in volume 1 and L_v is the minimum length from the piston to the constriction; see Figure 2.

Several assumptions are made to simplify the calculations. Those assumptions are needed to decrease the calculation time in the time-domain simulations and were used by Bodén [33, 34] to derive time-variant impedances. But when using the harmonic balance technique, it is easy to incorporate more complicated models. Therefore an effort is made here to replace the most questionable assumptions.

For example, the assumptions of continuous volume flow and continuous mass flow from one side to the other side of volume 2 are redundant. In the assumptions it is stated that the density in the constriction ρ_2 is constant while the densities ρ_1 in volume 1 and ρ_3 in volume 3 have time dependence. Then the assumption of continuity in volume flow implies that there is no time difference between the pressures P_1 and P_3. But the stiff mass plug in the constriction implies a time difference, and the assumptions are found to be contradictory.

An oscillating volume flow of course implies that there is zero flow at some specific times. In such cases and for very low flow velocity, no jet is formed at the outlet [37]. In the case with jet formation, the diameter of the constriction will be a time dependent *vena contracta* [38].

Following the discussion above, it is desirable to extend the model to include more subtle effects.

2.3. THE EXTENDED MODEL

Here the condition of continuous volume flow in junctions is replaced. To this end, equation (11) is rewritten as three separate equations,

$$\frac{\mathrm{d}}{\mathrm{d}t}(V_1(t)\rho_1(t)) = -\rho_2 Q_2(t), \tag{15}$$

$$\rho_1(t)Q_1(t) = \rho_2 Q_2(t), \qquad \rho_2 Q_2(t) = \rho_3(t)Q_3(t). \tag{16, 17}$$

Note that the time dependence explicitly has been written to separate the constant density ρ_2 form the time-varying quantities. The density $\rho_3(t)$ and the pressure $P_3(t)$ are furthermore supposed to have an adiabatic flow dynamical relationship, that is,

$$P_3 = P_0(\rho_3/\rho_0)^n. \tag{18}$$

By combining these equations with conservation of momentum one obtains the extended model:

$$P_1 - P_3 = \begin{cases} \dfrac{\rho_1}{2}\left[\dfrac{\rho_3^2 Q_3^2}{\rho_2^2 S_2^2} - \dfrac{\rho_3^2 Q_3^2}{\rho_1^2 S_1^2}\right] + \dfrac{\delta_1 + l_2}{S_2}\dfrac{\mathrm{d}}{\mathrm{d}t}(\rho_3 Q_3), & Q_3 > 0 \\ -\dfrac{\rho_3}{2}\left[\dfrac{\rho_3^2 Q_3^2}{\rho_2^2 S_2^2} - \dfrac{Q_3^2}{S_3^2}\right] + \dfrac{\delta_3 + l_2}{S_2}\dfrac{\mathrm{d}}{\mathrm{d}t}(\rho_3 Q_3), & Q_3 < 0 \end{cases} \tag{19}$$

$$\frac{\mathrm{d}}{\mathrm{d}t}(V_1\rho_1) = -\rho_3 Q_3, \qquad Q_3(\omega) = Y_3(\omega)P_3(\omega), \tag{20, 21}$$

$$P_1 = P_0(\rho_1/\rho_0)^n, \tag{22}$$

$$P_3 = P_0(\rho_3/\rho_0)^n, \tag{23}$$

where the time dependence once again has been omitted. Equations (19–23), now define the extended model.

3. THE SOLUTIONS OBTAINED WITH THE HARMONIC BALANCE

3.1. THE HARMONIC BALANCE METHOD (HBM)

3.1.1. *The method and some applications*

The HBM is a technique used on systems including both linear and non-linear parts. The fundamental idea of HBM is to decompose the system in two separate subsystems, a linear part and a non-linear part. The linear part is treated in the frequency domain and the non-linear part in the time domain. The interface between the subsystems consists of the Fourier transform pair. Harmonic balance is said to be reached when a chosen number of harmonics N satisfy some predefined convergence criteria. First, an appropriate unknown is chosen to use in the convergence check, which is performed in the frequency domain. Then the equations are rewritten in a suitable form for a convergence loop; see for example Figure 5. One starts with an initial value of the chosen unknown, applies the different linear and non-linear equations, and finally reaches a new value of the chosen unknown. If the difference between the initial value and the final value of the first N harmonics satisfy the predefined convergence criteria, harmonic balance is reached. Otherwise, an increment of the initial value is calculated by using a generalized Euler method, namely the Newton–Raphson method.

It should be mentioned that HBM is similar to other proposed coupling techniques, but one advantage of HBM is the calculation of the increment of the initial value. The method proposed by Gupta and Munjal [15] also includes an iterative process with a convergence condition. The main difference between their method and the HBM is how the chosen convergence unknown is treated. In HBM one calculates an increment which depends on the difference of the value at the beginning of the convergence loop and the final value after the loop. This implies a faster and more robust convergence. In the method of Gupta and Munjal, the final value is entered as a new initial value, which easily leads to slower convergence or divergence.

The method has been adopted successfully earlier for self-sustained oscillations of musical wind instruments [22]. The method was found to be very convenient for showing the modifications of the playing frequency and the spectrum when a physical parameter was changed or a new term was introduced in the equations.

In the applications of Nakhla *et al.* [20] the HBM is used as a practical and effective method to analyze the steady state regimes based on the use of voltage and current probes of non-linear microwave circuits. The stability of the periodic solutions reached can be studied as well [23].

To apply an inverse transformation, a sum of sines and cosines which converts the frequency domain data to time-domain data was used. Let ω be the fundamental angular frequency and N the truncated number of harmonics considered.
If $X(\omega) = FT\{x\} = \{C_k\}$, where FT means the Fourier transform, then

$$x(t) = \sum_{k=1}^{N} C_k e^{ik\omega t} = \sum_{k=1}^{N} [a_k \cos(k\omega t) + b_k \sin(k\omega t)]. \tag{24}$$

The relation between a_k, b_k and C_k is given by $C_k = (a_k - ib_k)/2$.

In the final equations of the model, the equations adopted to the HBM convergence loop, one has both integrals and derivatives. One of the advantages of the HBM is that

it is very easy to integrate and derive. If the variable is given by equation (24), then the integral is

$$\int x(t)\,\mathrm{d}t = \int \sum_{k=1}^{N} [a_k \cos(k\omega t) + b_k \sin(k\omega t)]\,\mathrm{d}t$$
$$= \sum_{k=1}^{N} \left[\frac{a_k}{k\omega} \sin(k\omega t) - \frac{b_k}{k\omega} \cos(k\omega t) \right] + C.$$

The constant C has to be determined by some appropriate condition. For the derivative one obtains

$$\frac{\mathrm{d}x}{\mathrm{d}t} = \frac{\mathrm{d}}{\mathrm{d}t} \sum_{k=1}^{N} [a_k \cos(k\omega t) + b_k \sin(k\omega t)]$$
$$= \sum_{k=1}^{N} [-a_k k\omega \sin(k\omega t) + b_k k\omega \sin(k\omega t)].$$

This implies that the numerical values of the derivatives and integrals are as accurate as the numerical value of the variable.

3.1.2. *HBM applied to the cold engine model*

To avoid numerical problems such as cancellation and different magnitudes of the unknowns, one can transform the equations to corresponding dimensionless equations. The standard transformation for non-linear acoustics is used for the quantities with non-zero mean values and for Q_3 a non-standard transformation is used. One has

$$P_1 = P_0(1 + M_a P_{1a}), \qquad P_3 = P_0(1 + M_a P_{3a}), \qquad \rho_1 = \rho_0(1 + M_a \rho_{1a}),$$
$$V_1 = V_{1m}(1 + M_a V_{1a}), \qquad Q_3 = V_{1m} f M_a Q_{3a},$$

where $M_a = u_a/c_0$ is the acoustical Mach number close to the piston and V_{1m} is the mean value of volume 1; see Figure 2. Here u_a is set to the velocity of the piston. Equations (10–12) are now rewritten in the new dimensionless unknowns and adopted to the chosen HBM convergence loop. Note that the admittance relation is applied in dimensional variables. Equations (10) becomes

$$P_{3a} = \begin{cases} P_{1a} - A\left(\dfrac{1}{S_2^2} - \dfrac{1}{S_1^2}\right) Q_{3a}^2 - B(\delta_1 + l_2)\dfrac{\mathrm{d}Q_{3a}}{\mathrm{d}t}, & Q_{3a} > 0 \\ P_{1a} + A\left(\dfrac{1}{S_2^2} - \dfrac{1}{S_3^2}\right) Q_{3a}^2 - B(\delta_3 + l_2)\dfrac{\mathrm{d}Q_{3a}}{\mathrm{d}t}, & Q_{3a} < 0 \end{cases} \tag{25}$$

where

$$A = \omega^2 \rho_0 V_{1m}^2 M_a / 2^3 \pi^2 P_o \quad \text{and} \quad B = \frac{\omega V_{1m} \rho_0}{2\pi P_0 S_2}.$$

For equations (11) and (12) one obtains

$$\rho_{1a} = -\frac{\omega}{2\pi(1 + M_a V_{1a})} \int Q_{3a}\,\mathrm{d}t - \frac{1}{M_a}, \quad \text{and} \quad P_{1a} = \frac{(1 + M_a \rho_{1a})^n - 1}{M_a}. \tag{26, 27}$$

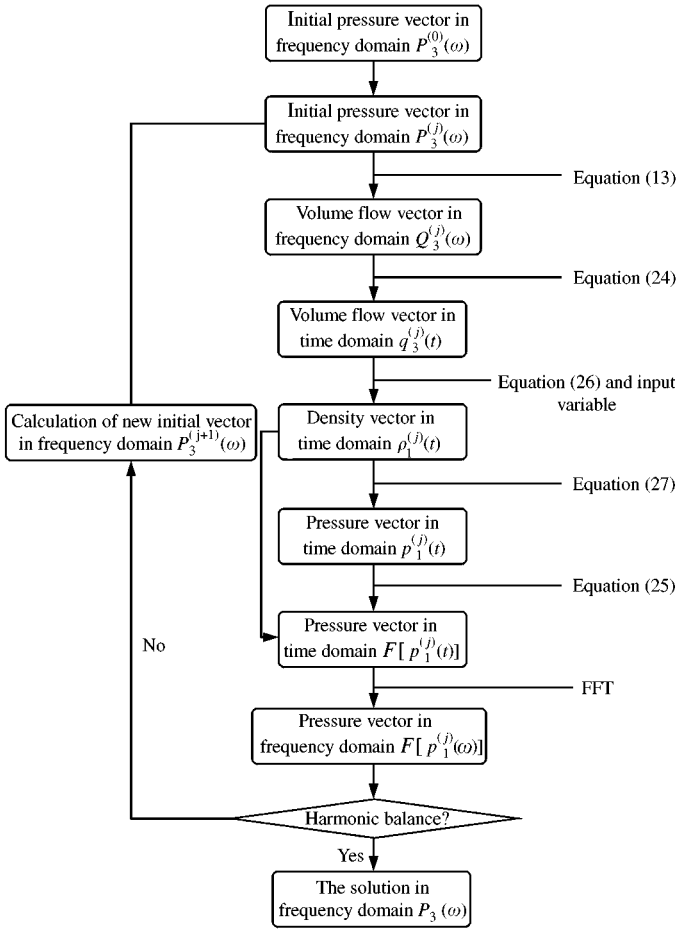

Figure 5. The harmonic balance convergence loop.

The convergence loop is given in Figure 5. The chosen convergence unknown is the pressure $P_{3a}^{(j)}(\omega)$ just after the outlet of the restriction, where the superscript j denotes that it is iteration number j. The equations are applied according to Figure 3; see Appendix B1 for more details. Finally, a new value of the convergence unknown is calculated, i.e., $F[P_{3a}^{(j)}(\omega)]$. This value is compared with $P_{3a}^{(j)}(\omega)$ for the first N harmonics in the frequency domain. If the difference satisfies the specified convergence criteria, the solution is obtained. Otherwise, an increment to the initial vector $P_{3a}^{(j)}(\omega)$ is calculated by

$$P_{3a}^{(j+1)}(\omega) = P_{3a}^{(j)}(\omega) - J_{P_{3a}}^{-1}\{P_{3a}^{(j)}(\omega) - F[P_{3a}^{(j)}(\omega)]\},$$

where $J_{P_{3a}}$ is the Jacobian matrix of the function $P_{3a}^{(j)}(\omega) - F[P_{3a}^{(j)}(\omega)]$. The calculation process is now repeated by calculating $F[P_{3a}^{(j+1)}(\omega)]$ from the new initial vector $P_{3a}^{(j+1)}(\omega)$, until convergence is reached.

3.1.3. *Comparison with time-domain simulations*

It is of course important to check the results from the harmonic balance method with results of alternative methods. To this end the solution obtained by using one of Matlab's

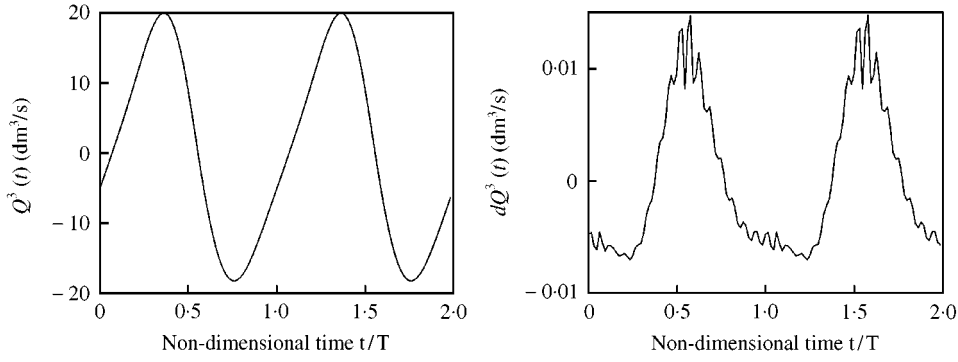

Figure 6. The volume flow $Q_3(t)$ and the difference between the time-domain simulation and the harmonic balance method $dQ_3(t)$ for driving frequency $f = 20$ Hz, $L_v = 0{\cdot}36$ m, $L_2 = 0{\cdot}02$ m and an infinite acoustic load pipe.

ordinary differential equation solvers in the time domain has been calculated; see Appendix A for further details. The comparison case is chosen to be an infinite pipe since one does not have to calculate a convolution integral in that case. Thus, only the characteristic impedance is considered. As seen in Figure 6 the results from the harmonic balance method are almost equivalent to the time-domain simulation results for the case with an infinite pipe. Note that the figure on the left-hand side is the HBM solution and that the Figure on the right shows the difference between the HBM and the time-domain solutions (the difference is always less than 0·1%). The time required for calculating the solution by using the time-domain method on a portable Pentium 166 MHz is several hours. With the HBM, the corresponding calculation takes around 1 min on the same PC.

3.2. RESULTS FROM THE HBM AND DISCUSSION

3.2.1 *Results from the basic model*

The convergence criteria used in the presented numerical simulations give a correct spectrum interval of 80 dB. This means that the limit of the correct spectra is 80 dB below the highest peak.

Figure 7 is an example of the results obtained by the HBM. It is easy to extract the wanted unknown when the solution has converged. The sound pressure level of P_3 as a function of the harmonic number, as well as the acoustic pressure P_3 are plotted. It is clear that the wave shapes include several other harmonic frequencies compared to the oscillating volume. This is a sign of the non-linearities in the system equations. Note that the sound pressure level is plotted as a function of harmonics in the frequency domain. From HBM one always gets harmonics of the fundamental frequency, which is $f = 10$ Hz in Figure 7. To include for example, half harmonics a fundamental frequency of twice the harmonic frequency has to be applied. Then all half harmonics are found as well.

In the engine model of Boonen [27, 28] the pressure at the outlet of the engine manifold is calculated. Figure 8 shows the pressure $P_3(t)$ for a certain parameter configuration. The in-duct pressure P_3 then corresponds to the induct pressure of Boonen just after the engine manifold. A comparison of this figure to corresponding figures in references [27, 28] shows that this simple piston restriction model can approximate the sound pressure of an engine. If the parametric study of a system would take a long time and be a heavy process, the

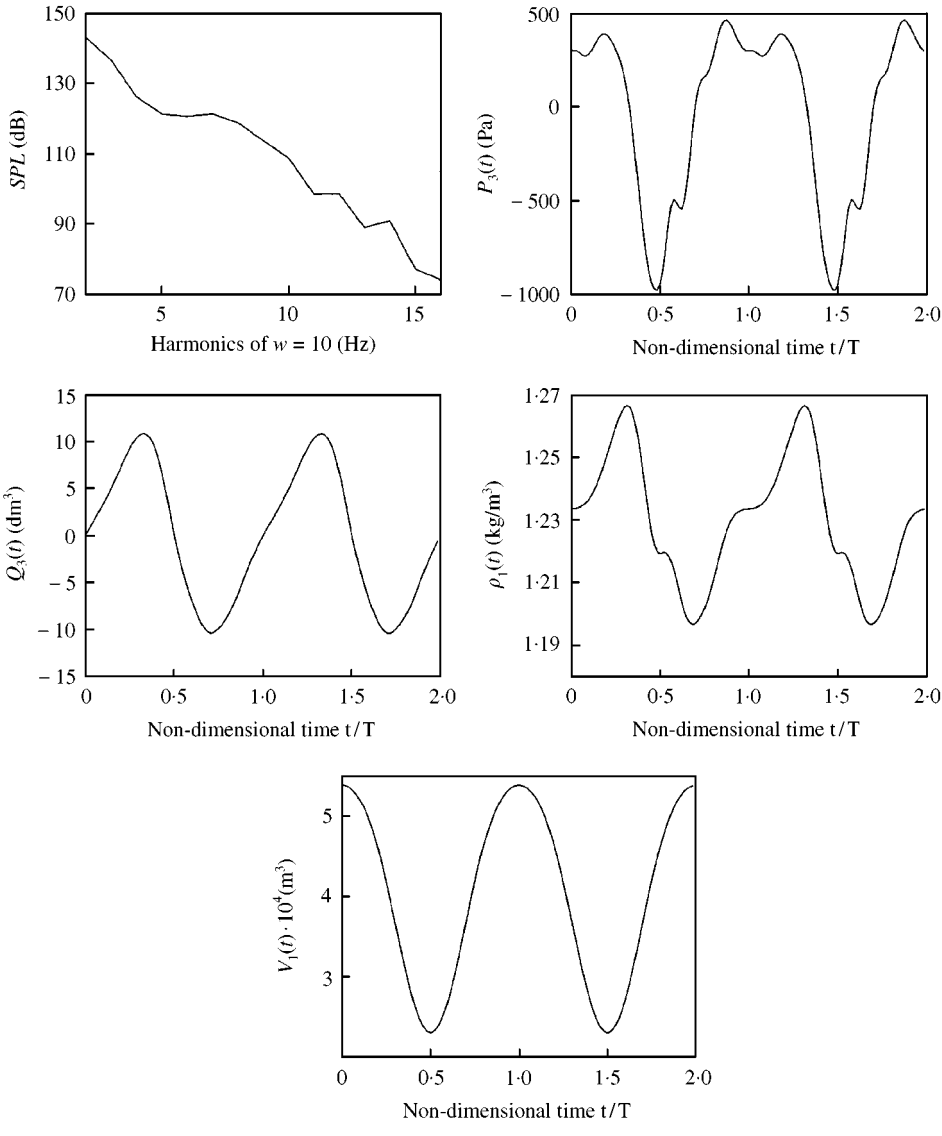

Figure 7. The sound pressure level (SPL) of P_3 as a function of the harmonic number, the pressure P_3, the volume flow Q_3, the density ρ_1 and the volume V_1 as functions of time plotted for two periods. The model parameters used are $L_v = 0{\cdot}06$ m, $L = 1{\cdot}1$ m, $d_2 = 0{\cdot}013$ m, $l_2 = 0{\cdot}02$ m and $f_0 = 10$ Hz.

possibility to find suitable parameters of the system would be limited. But the HBM is a fast and simple method to find appropriate parameters for certain wave shapes or some other required properties that are shown in Figure 7.

As stated above, one major advantage with the HBM is the possibility to perform parametric studies very easily. Here some examples of parametric studies are presented to show the ability of the method and to draw conclusions about the model used. In Figure 9, the internal pressure P_3 plotted as a function of time as well as the sound pressure level of the same variable are shown. Only the length L_v, viz., the minimum length from the piston to the constriction, is varied.

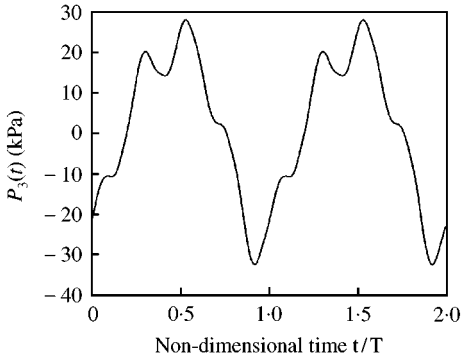

Figure 8. The in-duct sound pressure $P_3(t)$ for comparison with results from Boonen.

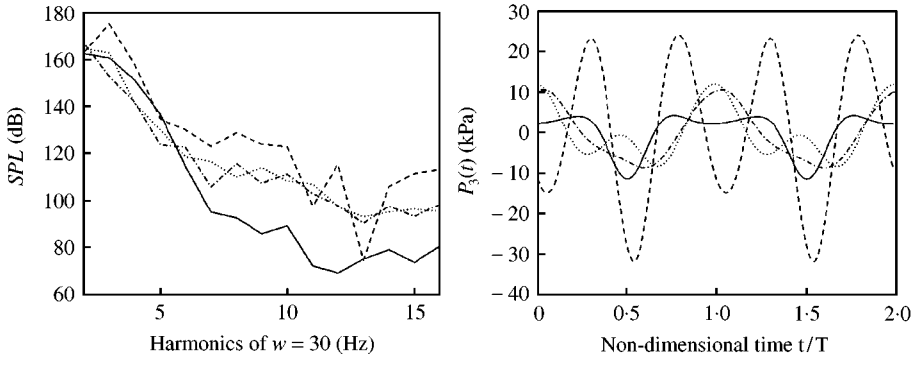

Figure 9. The sound pressure level of P_3 as a function of the harmonic number and the pressure P_3 as a function of time. Here only the distance L_v is varied; see Figure 1. The different distances are $L_v = 0{\cdot}01$ m (——), $L_v = 0{\cdot}10$ m (– – – –), $L_v = 0{\cdot}20$ m (·····) and $L_v = 0{\cdot}40$ m (– · – · – · –). The parameters used are $d_2 = 0{\cdot}03$ m, $l_2 = 0{\cdot}02$ m, $L = 1$ m, $f_0 = 30$ Hz.

It is obvious that the choice of L_v is crucial to the sound generated in the pipe. Note that the case with minimum distance to the constriction does not give largest pressure. In Figure 10 only the diameter d_3 of the pipe is varied.

In Figure 11, only the diameter d_2 of the constriction is varied and one can see a large difference between the curves. Following the discussion about the assumption at the end of section 2.2 a model including the time-varying diameter of the constriction would probably significantly influence the results.

The parametric study of the variation of the constriction length in Figure 12 shows that the influence of the length l_2 is less than the influence of the diameter d_2. But one can still see significant differences between the solutions of system with different lengths of the constriction. Since it is easy to include additional terms in the HBM with only a minor increase of calculation time, it would be possible to include this effect as well.

The non-linear effects of the system are clearly shown when only the amplitude is varied. If the system were linear, a variation of amplitude would only change the amplitude of the results. In Figure 13 the relative amplitude is varied from 1 to 1·3; see Figure 2 and equation (14) for a detailed description of the piston movement. In all three quantities, viz.,

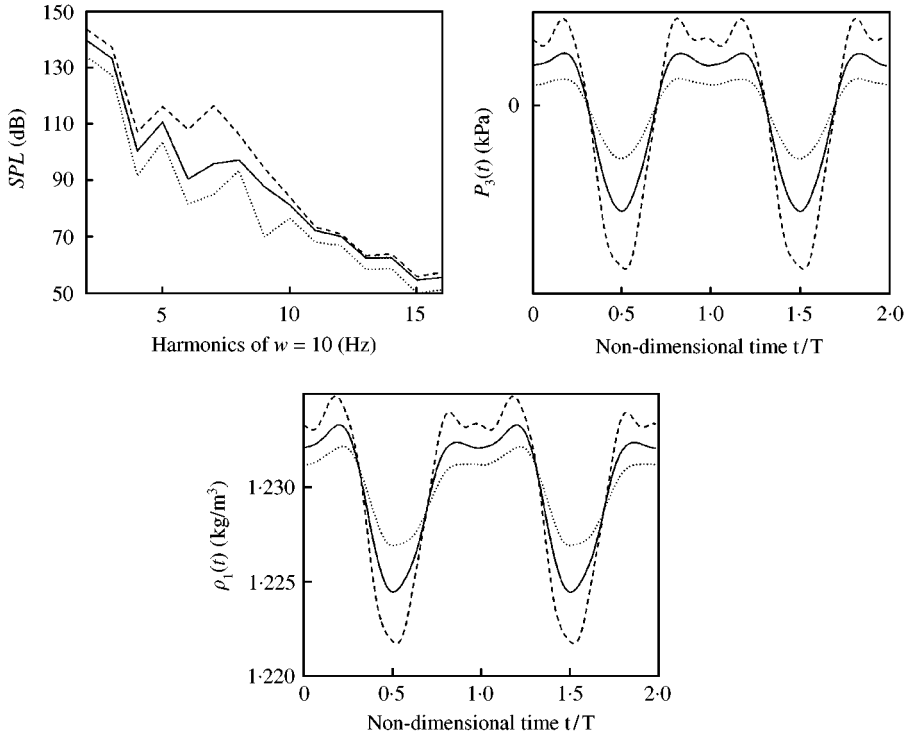

Figure 10. The sound pressure level of P_3 as a function of the harmonic number, the pressure P_3 and the density ρ_1 as functions of time. Here only the diameter d_3 of the pipe is varied, see Figure 1. The different diameters are $d_3 = 0{\cdot}07$ m (·····), $d_3 = 0.05$ m (——) and $d_3 = 0{\cdot}04$ m (– – – –). The parameters used are $d_2 = 0{\cdot}03$ m, $L_v = 0{\cdot}10$ m, $l_2 = 0{\cdot}02$ m, $L = 1$ m, $f_0 = 10$ Hz.

the internal pressure $P_3(t)$, the volume flow $Q_3(t)$ and the density $\rho_1(t)$, the difference is clear. When the amplitude is increased, the amplitudes and the shapes of the curves change. Thus it is shown that the source part is allowed to vary non-linearly while using the HBM with a linear acoustic load system given by an impedance/admittance.

3.2.2. *Results from extended models*

In this section the results from the two different source models are compared by using the HBM. The basic source model given by equations (10–13) and the extended source model given by equations (19–23) are used in the HBM with exactly the same parameters for three different parameter sets. The first set represents a system with a small non-linearity. That is, a restriction with large diameter is used, the amplitude of the driving piston is reduced to half of its value compared to the actual piston and the oscillating volume has a large mean value. The second set represents a medium non-linearity. Here, the restriction diameter is reduced, the amplitude of the piston is restored and the mean value of the oscillating volume is reduced. Finally, the third set is chosen to create quite a large non-linearity in the system. To this end, the diameter of the restriction as well as the mean value of the oscillating volume are reduced even further.

Figure 14 shows that for almost linear systems we have a very small difference between the basic model and the extended model. It is therefore suitable to use the basic model for almost linear systems. Maybe it is even possible to use the linear time-invariant source

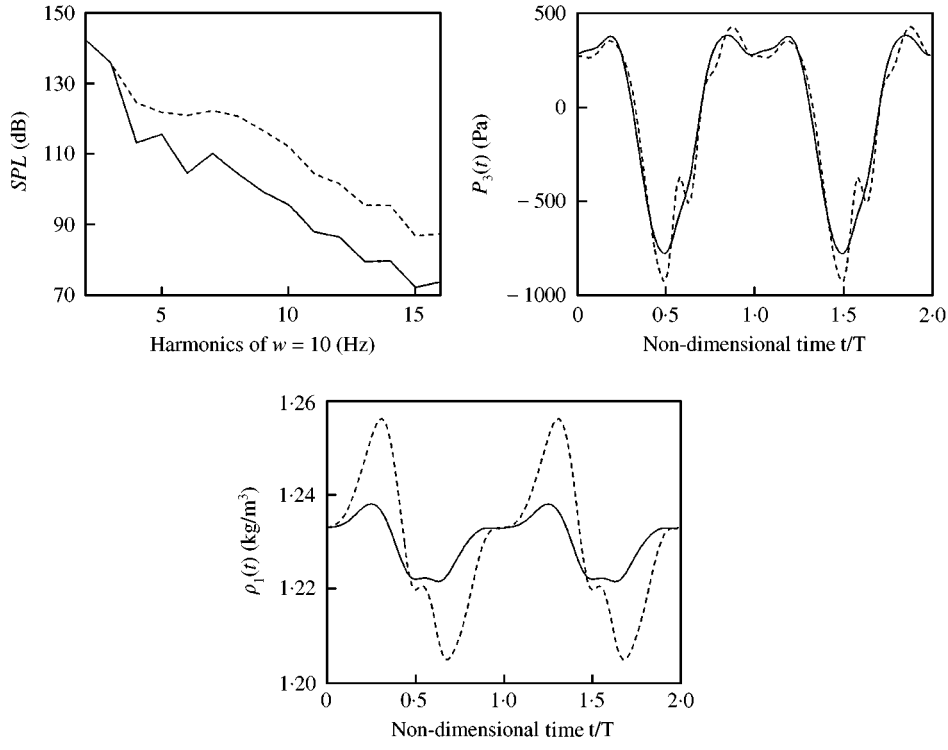

Figure 11. The sound pressure level of P_3 as a function of the harmonic number, the pressure P_3 and the density ρ_1 as functions of time. Here only the diameter d_2 is varied; see Figure 1. The different diameters are $d_2 = 0{\cdot}02$ m (——) and $d_2 = 0{\cdot}02/\sqrt{2}$ m (– – – –). The parameters used are $L_v = 0{\cdot}10$ m, $l_2 = 0{\cdot}02$ m, $L = 1$ m, $f_0 = 10$ Hz.

model. For the medium non-linearity given in Figure 15 as well as for the large non-linearity given in Figure 16 there are clear discrepancies between the basic and the extended model.

For these cases, a better description is gained by using the extended source model. An even better description would be possible if a time-varying constriction diameter, viz., *vena contracta* [38], as well as the fact that the flow does not form a jet at the outlet for all cases [37], were taken into account in the model.

4. CONCLUSION AND DISCUSSION

The proposed method for calculating the time–frequency domain coupling is found to have several advantages. One can easily perform parametric studies by varying one specific parameter at a time; see Figure 13. The calculation time is short and it is easy to extract the behaviour of the required unknown when the specific parameter is varied. By changing the fundamental frequency compared to the driving frequency of the oscillator, one could include half order, on third orders and so on.

The main disadvantage with the HBM is that only periodic solutions are studied. One cannot find any transient solutions, which are of great interest in industry applications. The method is, however, useful in a lot of industrial applications, since it permits the sound source to respond differently to different applied pipe/muffler systems. HBM could be used together with commercial linear acoustic simulation programs, for example SID [39], to provide the coupling between the source and the exhaust and intake systems.

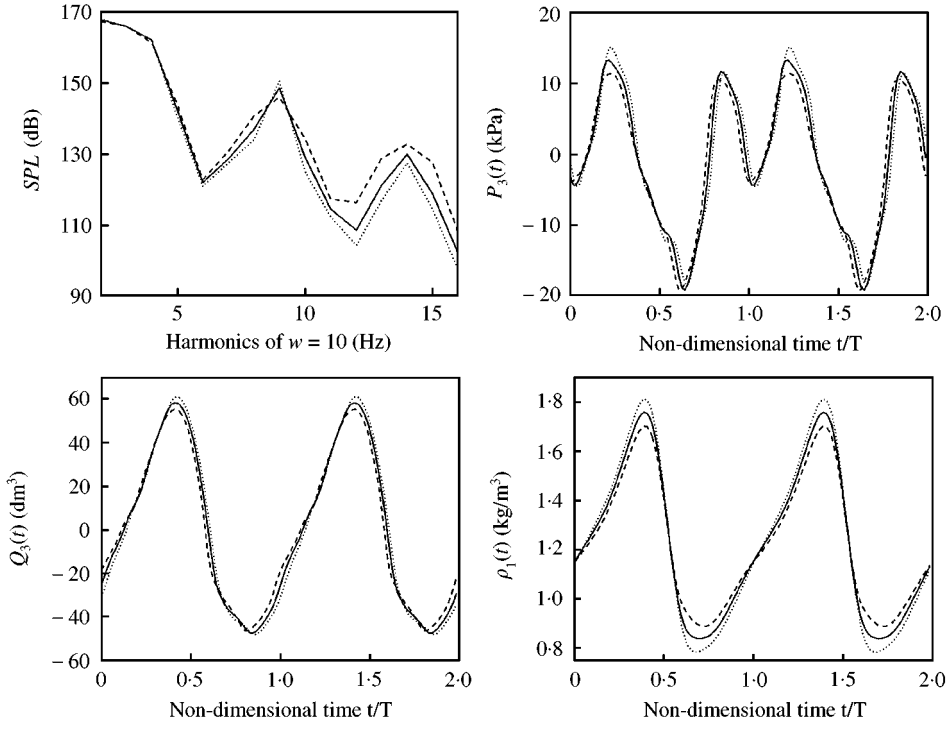

Figure 12. The sound pressure level of P_3 as a function of the harmonic number, the pressure P_3, the volume flow Q_3 and the density ρ_1 as functions of time. Here only the length of the constriction l_2 is varied; see Figure 1. The different lengths are $l_2 = 0{\cdot}10$ m (·····), $l_2 = 0{\cdot}06$ m (——) and $l_2 = 0{\cdot}01$ m (– – – –). The parameters used are $d_2 = 0{\cdot}015$ m, $L_v = 0{\cdot}05$ m, $L = 0{\cdot}65$ m, $f_0 = 50$ Hz.

This paper is a first step in the modelling of a "one-cylinder cold engine". The emphasis has therefore not been to tune the model, i.e., the equations, but to find an appropriate method, which can be used for the coupling between the time domain and frequency domain. Since the HBM was found to be an efficient tool for the periodic regimes, the next step is to improve the engine model, and finally to conduct some measurements. This is, however, out of the scope of this paper.

Further research is needed in areas of different coupling methods and source models to be used with the linear simulation codes of the industry. It would also be interesting to further develop the linearity tests proposed in reference [19]. The objectives would be to find a simple test from which it can be determined qualitatively which required the degree of complexity for the source model. That is, if the linear model is sufficient, if a hybrid model or if a fully non-linear model is needed.

Another interesting future subject is to include the effects of mean flow in the model. This would make it possible to use the model together with HBM as a design tool to balance the requirements for good flow performance and low noise.

The results from the HBM can furthermore be used as an input to a perturbation method for including non-linear wave propagation in the pipes.

ACKNOWLEDGMENTS

This work was done within the EC-project FLODAC under contract no: BRPR CT97-0394. The authors wish to thank Yves Auregan, Hans Bodén and Jean Kergomard for useful comments on the paper.

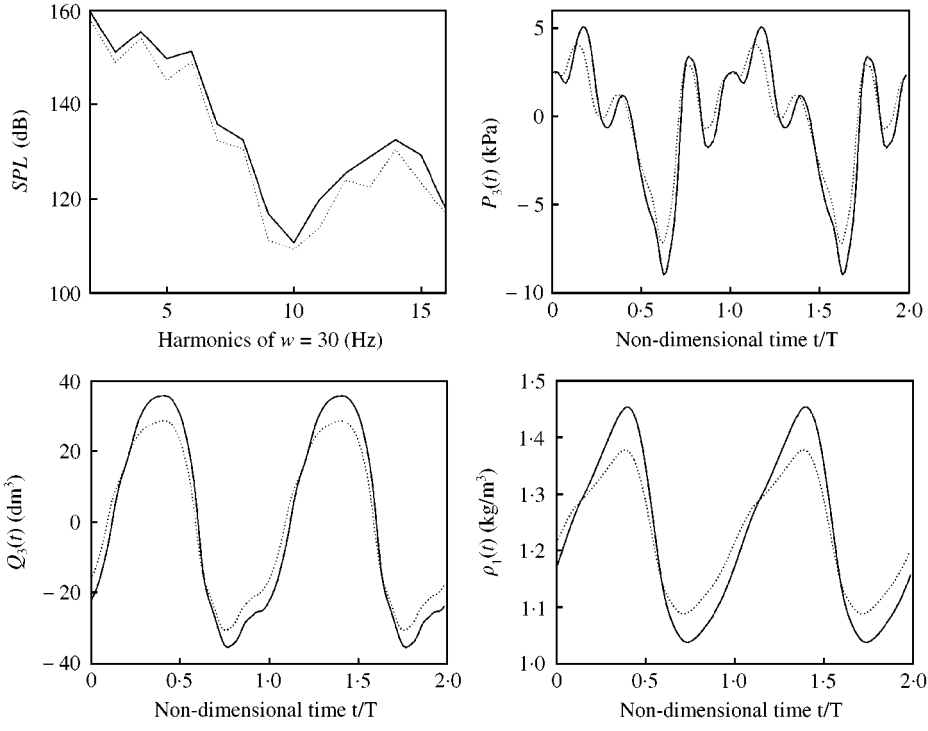

Figure 13. The sound pressure level of P_3 as a function of the harmonic number, the pressure P_3, the volume flow Q_3 and the density ρ_1 as functions of time. Here the relative amplitude is varied from 1 (·····) to 1·3 (——). Here $L_v = 0{\cdot}16$ m, $L = 0{\cdot}65$ m, $d_2 = 0{\cdot}015$ m, $l_2 = 0{\cdot}02$ m and $f_0 = 30$ *Hz*.

REFERENCES

1. L. Desmons and J. Kergomard 1994 *Applied Acoustics* **41**, 127–155. Simple analysis of exhaust noise produced by a four cylinder engine.
2. A. D. Jones 1984 *Noise Control Engineering Journal* **23**, 12–31. Modelling the exhaust noise radiated from reciprocating internal combustion engines—a literature review.
3. A. D. Jones and G. L. Brown 1982 *Journal of Sound and Vibration* **148**, 437–453. Determination of two-stroke engine exhaust noise by the method of characteristics.
4. G. Ferrari and R. Castelli 1985 *Noise Control Engineering Journal* **24**, 50–56. Computer predictions and experimental tests of exhaust noise in a single cylinder internal combustion engine.
5. S. M. Sapsford, V. C. M. Richards, D. R. Amlee, T. Morel and M. T. Chapell 1992 *Society of Automotive Engineering Paper No*. 920686. Exhaust system evaluation and design by non-linear modelling.
6. F. Payri, A. J. Torregrosa and M. D. Chust 1996 *Journal of Sound and Vibration* **195**, 757–773. Application of MacCormack schemes to I.C. engine exhaust noise prediction.
7. F. Payri, A. J. Torregrosa and A. Broatch 1997 *Society of Automotive Engineering Paper No*. 970836. A numerical study of the behaviour of a turbocharged diesel engine as a noise source.
8. M. L. Munjal 1998 *Journal of Sound and Vibration* **211**, 425–433. Analysis and design of mufflers—an overview of research at the Indian Institute of Science.
9. K. R. Norman, A. Selamet and J. M. Novak 1998 *Journal of Sound and Vibration* **218**, 711–734. Perforated muffler manifold catalyst.
10. P. A. O. L. Davies and M. F. Harrison 1997 *Journal of Sound and Vibration* **202**, 249–274. Predictive acoustic modelling applied to the control of intake/exhaust noise of internal combustion engines.
11. H. Bodén and M. Åbom 1995 *Acta Acustica* **3**, 549–560. Modelling of fluid machines as sources of sound in duct and pipe systems.

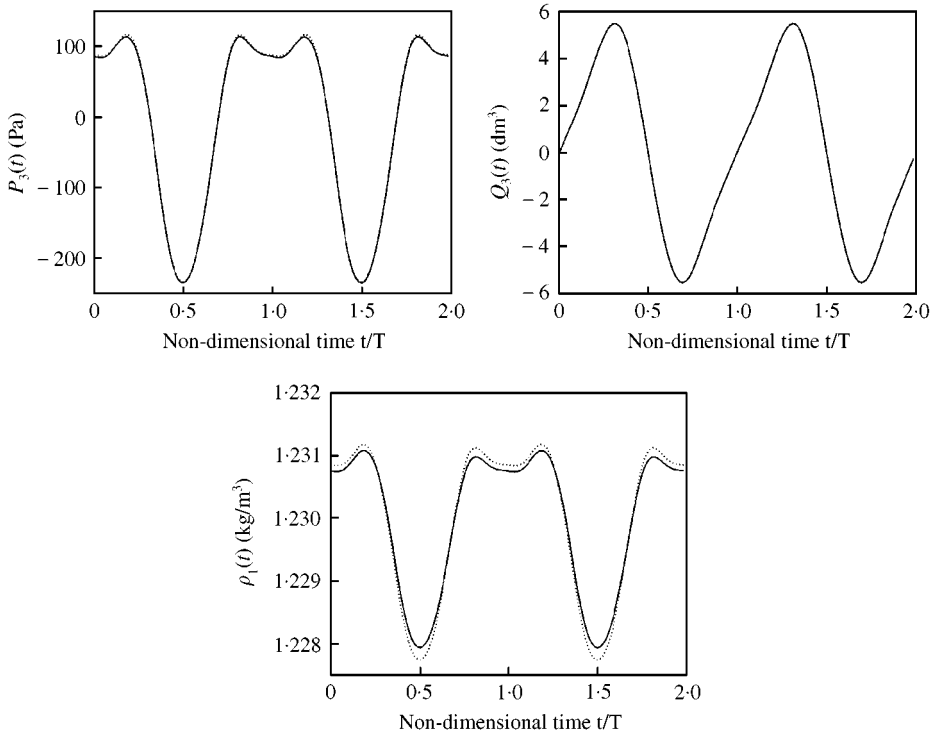

Figure 14. The pressure P_3, the volume flow Q_3 and the density ρ_1 as functions of time, for a slightly non-linear system: ·····, basic model; ——, extended model.

12. H. BODÉN 1997 *Report TRITA-FKT*-9735, KTH, Stockholm, Sweden. Measurement of acoustic source data for truck engines: Part 1.
13. F. ALBERTSON 1998 *Report TRITA-FKT* 1998:14, KTH, Stockholm, Sweden. Measurement of acoustic source data for truck engines: Part 2.
14. F. ALBERTSON and H. BODÉN 1999 *Report TRITA-FKT* 1999:22, KTH, Stockholm, Sweden. Measurement of acoustic source data for truck engines: Part 3.
15. V. H. GUPTA and M. L. MUNJAL 1992 *Journal of the Acoustical Society of America* **92**, 2716–2725. On numerical prediction of the acoustic source characteristics of an engine exhaust system.
16. J. M. DESANTES, A. J. TORREGROSA and J. P. BRUNEL 1995 *Society of Automotive Engineering Paper No.* 950545. Hybrid linear/nonlinear method for exhaust noise prediction.
17. P. O. A. L. DAVIES and K. R. HOLLAND 1999 *Journal of Sound and Vibration* **223**, 425–444. I. C. engine intake and exhaust noise assessment.
18. J. LAVRENTJEV, H. BODÉN and M. ÅBOM 1992 *Journal of Sound and Vibration* **155**, 534–539. A linearity test for acoustic one-port sources.
19. H. BODÉN and F. ALBERTSON 2000 *Journal of Sound and Vibration* **237**, 45–65. Linearity tests for in-duct acoustic one-port sources.
20. M. S. NAKHLA and J. VLACH 1976 *IEEE Transactions on Circuit Theory* **23**, 85–91. A piece-wise harmonic balance technique for determination of periodic response of nonlinear systems.
21. E. NGOYA, J. ROUSSET, M. GAYRAL, R. QUERE and J. OBREGON 1990 *IEEE Transactions on Circuits and Systems* **37**, 1339–1355. Efficient algorithms for spectra calculations in nonlinear microwave circuits simulators.
22. J. GILBERT, J. KERGOMARD and E. NGOYA 1989 *Journal of the Acoustical Society of America* **86**, 35–41. Calculation of the steady-state oscillations of a clarinet using the harmonic balance technique.
23. E. NGOYA, A. SUAREZ, R. SOMMET and R. QUERE 1995 *International Journal of Microwave and Millimeter Wave and Computer-Aided Engineering* **5**, 210–223. Probes make simple the steady state analysis of microwave free or forced oscillator and the stability investigation of periodic regimes by harmonic balance.

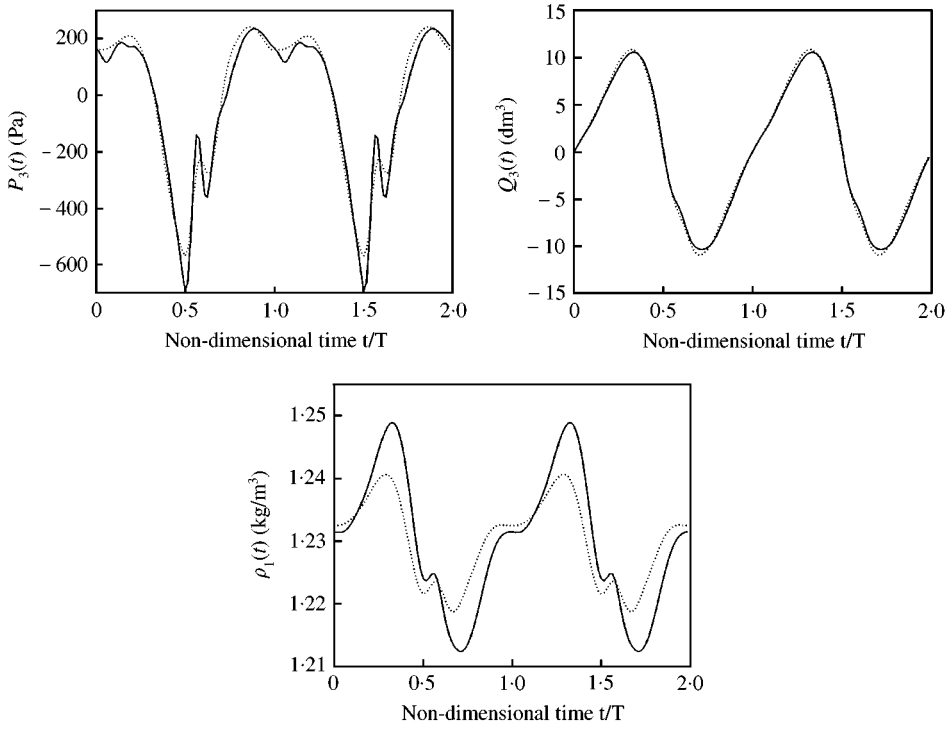

Figure 15. The pressure P_3, the volume flow Q_3 and the density ρ_1 as functions of time, for a medium non-linear system: ·····, basic model; ——, extended model.

24. F. PAYRI, J. M. DESANTES and A. J. TORREGROSA 1995 *Journal of Sound and Vibration* **188**, 85–110. Acoustic boundary condition for unsteady one-dimensional flow calculations.
25. J. B. HEYWOOD 1988 *Internal Combustion Engine Fundamentals*. New York: McGraw-Hill.
26. N. WATSON, A. D. PILLEY and M. MARZOUK 1980 *Society of Automotive Engineering Paper No.* 800029. A combustion correlation for diesel engine simulation.
27. R. BOONEN and P. SAS 1997 *Proceedings of the ACTIVE* 97 *Conference, Budapest*, 499–512. Design of an active noise cancellation device for internal combustion engines.
28. R. BOONEN and P. SAS 1999 *Proceedings of the ICSV* 99 *conference, Copenhagen*, 1635–1642. Design of an active controlled muffler for internal combustion engines.
29. B. R. C. MUTYALA and W. SOEDEL 1976 *Journal of Sound and Vibration* **44**, 479–491. A mathematical model of Helmholtz resonator type gas oscillation discharges of two-stroke cycle engines.
30. J. H. LEE and W. SOEDEL 1984 *Noise Control Engineering Journal* **24**, 19–37. On prediction of gas pulsations and exhaust noise of low amplitude pulse combustion systems.
31. J. J. NIETER and R. SINGH 1984 *Journal of Sound and Vibration* **97**, 475–488. A computer simulation study of compressor tuning phenomena.
32. J. H. LEE, B. DHAR and W. SOEDEL 1985 *Journal of Sound and Vibration* **98**, 379–401. A mathematical model of low amplitude pulse combustion systems using a Helmholtz resonator-type approach.
33. H. BODÉN 1988 *Report TRITA-TAK-8802, KTH, Stockholm, Sweden*. The multiple load method for measuring the source characteristics of time-variant sources.
34. H. BODÉN 1991 *Journal of Sound and Vibration* **148**, 437–453. The multiple load method for measuring the source characteristics of time-variant sources.
35. L. DESMONS 1992 *These de doctorat l'université du Maine, Le Mans, France*. Caractérisation acoustique d'un moteur quatre cylindres a combustion interne.

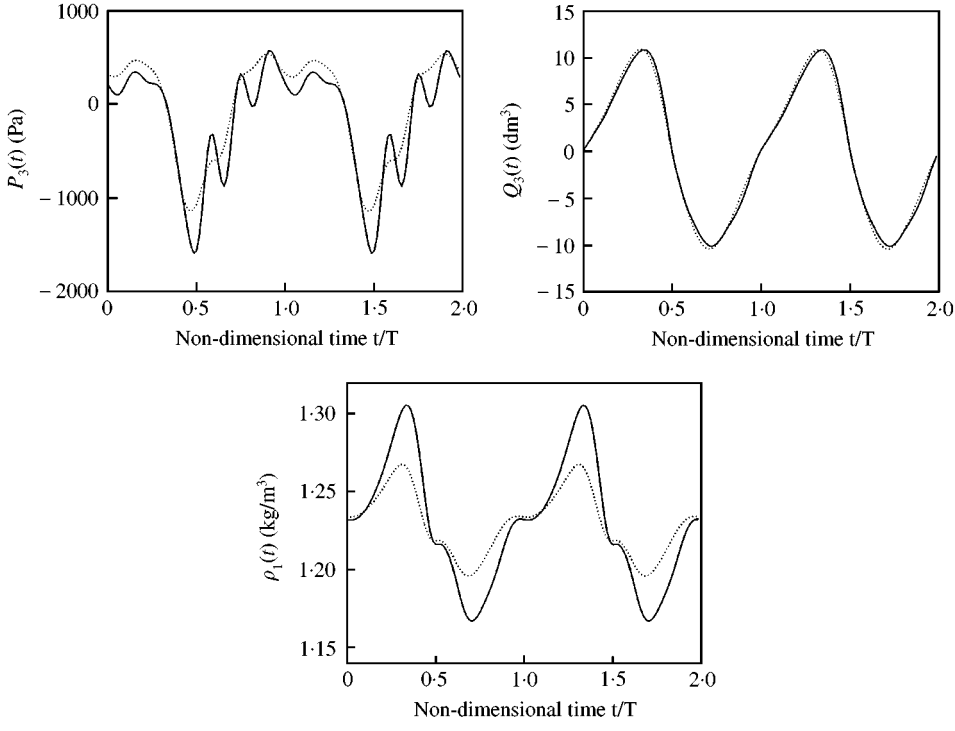

Figure 16. The pressure P_3, the volume flow Q_3 and the density ρ_1 as functions of time, for a largely non-linear system: ·····, basic model; ——, extended model.

36. J.-M. COULON 1994 *These de doctorat de l'université Paris* 6, *France*. Caractérisation de l'ensemble moteur collecteur comme source acoustique vis-à-vis de l'échappement des automobiles.
37. A. HIRSCHBERG, R. W. A. VAN DE LAAR, J. P. MARROU-MAURIÈRES, A. P. J. WIJNANDS, H. J. DANE, S. G. KRUIJSWIJK and A. J. M. HOUTSMA 1990 *Acustica* **70**, 146–154. A quasi-stationary model of air flow in the reed channel of single-reed woodwind instruments.
38. P. DURRIEU, G. HOFMANS, G. AJELLA, R. BOOT, Y. AUREGAN, A. HIRSCHBERG and M. C. A. M. PETERS 1999 *Journal of the Acoustical Society of America*. Quasi-steady aero-acoustic response of orifices (submitted).
39. R. GLAV 1990 *Report TRITA-TAK*-9002, *KTH*, *Stockholm*, *Sweden*. Analysis of the sound transmission properties of exhaust systems using the 4-pole method.

APPENDIX A: TIME-DOMAIN SOLUTIONS

For the time-domain simulation, equations (10–12) of the basic model are rewritten in a suitable form for using the Matlab predefined odesolver "ode45" with a variable steplength. Because of the hypothesis of an infinite pipe, equation (13) is only an equation of proportionality. That is, Y_3 does not depend on the frequency (characteristic admittance only). The solver "ode45" is a solver for non-stiff problems with medium accuracy, but as an option one can define small error tolerances to increase the accuracy. One define $y_1 = \rho_1 V_1$ and $y_2 = Q_3$ and keep the rest of the notations as above. The equations then become as follows. For y_1 one gets the differential equation

$$\frac{\mathrm{d}y_1}{\mathrm{d}t} = -\rho_0 Q_3.$$

For $Q_3 = y_2 > 0$,

$$\frac{\mathrm{d}y_2}{\mathrm{d}t} = \left[P_0 \left(\frac{y_1}{V_1 \rho_0} \right)^n - \frac{\rho_2 c_0 y_2}{S_3} - P_0 - \frac{\rho_0}{2} \left(\frac{1}{S_2^2} - \frac{1}{S_1^2} \right) y_2^2 \right] \frac{S_2}{\rho_0 (l_2 + \delta_1)},$$

and for $Q_3 = y_2 < 0$ one gets

$$\frac{\mathrm{d}y_2}{\mathrm{d}t} = \left[P_0 \left(\frac{y_1}{V_1 \rho_0} \right)^n - \frac{\rho_2 c_0 y_2}{S_3} - P_0 + \frac{\rho_0}{2} \left(\frac{1}{S_2^2} - \frac{1}{S_3^2} \right) y_2^2 \right] \frac{S_2}{\rho_0 (l_2 + \delta_3)}.$$

The ordinary non-linear differential equation system for the vector

$$\mathbf{y} = \begin{pmatrix} y_1 \\ y_2 \end{pmatrix}$$

is now solved by using "ode45". The results are given in Figure 4.

APPENDIX B: THE CONVERGENCE LOOPS FOR THE DIFFERENT SOURCE MODELS

B.1. THE BASIC MODEL

The convergence loop for the basic model, given by equations (10–13) is

$$P_3(\omega) \xrightarrow{\text{equation(13)}} Q_3(\omega) \xrightarrow{\text{equation(24)}} q_3(t) \xrightarrow{\text{equation(11)} + V_1(t)} \rho_1(t) \xrightarrow{\text{equation(12)}} p_1(t),$$

$$\left.\begin{matrix} q_3(t) \\ p_1(t) \end{matrix}\right\} \xrightarrow{\text{equation(10)}} F[p_3(t)] \xrightarrow{FFT} F[P_3(\omega)].$$

Note that all frequency domain variables are written with uppercase letters while the time-domain variables are represented by lowercase letters.

This convergence loop following Figure 5 is written as follows. The superscript j denotes that it is the iteration number j and the subscript a denotes that the dimensionless equations are used. The time dependence is omitted, but in the case of frequency dependence this is explicitly written. The initial value is chosen to be $P_3^{(j)}(\omega)$. The linear admittance relation (13) is applied to find $Q_{3a}^{(j)}(\omega)$, that is,

$$Q_3^{(j)}(\omega) = Y_3(\omega) P_3^{(j)}(\omega).$$

Now, the non-linear equations have to be applied in the time domain, so the sum in equation (24) gives

$$q_{3a}^{(j)} = \sum_{k=1}^{N} [a_k \cos(k\omega t) + b_k \sin(k\omega t)].$$

Equation (26) together with the input variable $V_{1a}(t)$ gives

$$\rho_{1a}^{(j)} = -\frac{\omega}{2\pi(1 + M_a V_{1a})} \int q_{3a}^{(j)}\, \mathrm{d}t - \frac{1}{M_a},$$

equation (27) gives

$$p_{1a}^{(j)} = \frac{(1 + M_a \rho_{1a}^{(j)})^n - 1}{M_a}.$$

Equation (25) gives

$$p_{3a}^{(j)} = \begin{cases} p_{1a}^{(j)} - A\left(\dfrac{1}{S_2^2} - \dfrac{1}{S_1^2}\right)(q_{3a}^{(j)})^2 - B(\delta_1 + l_2)\dfrac{\mathrm{d}q_{3a}^{(j)}}{\mathrm{d}t}, & q_{3a}^{(j)} > 0 \\ p_{1a}^{(j)} + A\left(\dfrac{1}{S_2^2} - \dfrac{1}{S_3^2}\right)(q_{3a}^{(j)})^2 - B(\delta_3 + l_2)\dfrac{\mathrm{d}q_{3a}^{(j)}}{\mathrm{d}t}, & q_{3a}^{(j)} < 0 \end{cases}$$

and finally by a Fourier transform one finds $F[P_{3a}^{(j)}(\omega)]$.

B.2. THE EXTENDED MODEL

For the extended model, given by equations (19–23), a slightly different convergence loop has to be used. Here one has

$$\left.\begin{array}{l} P_3(\omega) \xrightarrow{\text{equation(21)}} Q_3(\omega) \xrightarrow{\text{equation(24)}} q_3(t) \\ P_3(\omega) \xrightarrow{\text{equation(24)}} p_3(t) \xrightarrow{\text{equation(23)}} \rho_3(t) \end{array}\right\} \xrightarrow{\text{equation(20)} + V_1(t)} \rho_1(t) \xrightarrow{\text{equation(22)}} p_1(t),$$

$$\left.\begin{array}{l} p_1(t) \\ q_3(t) \\ \rho_1(t) \\ \rho_3(t) \end{array}\right\} \xrightarrow{\text{equation (19)}} F[p_3(t)] \xrightarrow{FFT} F[P_3(\omega)].$$

APPENDIX C: NOMENCLATURE

Each variable x is written $x(t)$ or x in the time domain and $x(\omega)$ in the frequency domain.

$P_0 = 10^5$	atmospheric pressure
$P_1(t)$	pressure in volume 1
$P_3(t)$	pressure in volume 3
$Q_1(t)$	volume flow in volume 1
$Q_2(t)$	volume flow in volume 2
$Q_3(t)$	volume flow in volume 3
$\rho_0 = 1{\cdot}23$	density of air
$\rho_1(t)$	density in volume 1
$\rho_2 = 1{\cdot}23$	density in volume 2
$\rho_3(t)$	density in volume 3

d_1	diameter of pipe 1
d_2	diameter of pipe 2
d_3	diameter of pipe 3
S_1	area of pipe 1
S_2	area of pipe 2
S_3	area of pipe 3
L_{A1}	length of axis in piston, see Figure 2
L_{A2}	length of axis in piston, see Figure 2
$V_1(t)$	oscillating volume
$n = 1{\cdot}4$	polytropic index